



HOW DRONES AND LIDAR HELP IN COUNTING MANGROVE TREES: A PRACTICAL APPROACH

Muhammad Rizki Nandika^{1*}, Jeverson Renyaan¹, Bayu Prayudha¹, La Ode Alifatri¹, Herlambang Aulia Rachman², Yaya Ihya Ulumuddin¹, Turissa Pragunanti Ilyas³, Dony Kushardono³, Martiwi Diah Setiawati^{1,4}

¹Research Center for Oceanography, National Research and Innovation Agency, B. J. Habibie Science and Technology Area (KST), Serpong, South Tangerang, 15314, Indonesia

²Department of Marine Science, University of Trunojoyo, Jl. Raya Telang, Bangkalan, 69112, Indonesia

³Research Center for Geoinformatics, National Research and Innovation Agency, Jl. Cisitu, Bandung, 40135, Indonesia ⁴United Nations University – Institute for the Advanced Study of Sustainability (UNU-IAS), 5-53-70 Jingumae,

Shibuya-ku, Tokyo, 150-8925, Japan

*Corresponding author: rizki.nandika@gmail.com

Received: March 18th 2025 / Accepted: June 23rd 2025 / Published: October 1st 2025

https://doi.org/10.24057/2071-9388-2025-3958

ABSTRACT. Mangrove forests provide critical ecosystem services, including coastal protection, habitat for biodiversity, and carbon sequestration. Monitoring these ecosystems is essential for their conservation and sustainable management. This study was conducted on Pramuka Island, Indonesia, focusing on high-density Rhizophora stylosa vegetation. Data was collected using the DJI M300 RTK UAV equipped with the Zenmuse L1 LiDAR sensor, which generated a Canopy Height Model (CHM) and identified treetops. Various kernel sizes (3×3, 5×5, 9×9, 11×11, 21×21) and Local Maximum Filter (LMF) window sizes (0.5, 1, 3 meters) were applied to analyze mangrove tree density. The study found that the combination of a 3×3 kernel with a 0.5 meter window size yielded the best results, achieving the highest F-score and balancing precision and recall. However, despite the optimized settings, LiDAR still struggled to detect individual trees in dense mangrove stands, resulting in the underestimation of tree counts compared to field data. This highlights the challenges LiDAR faces in dense vegetation environments. The study emphasizes the need for optimized kernel and window size configurations for more accurate tree detection and calls for further development of LiDAR-based algorithms to improve detection in mangrove forests. Improved methodologies will enhance the effectiveness of mangrove forest conservation and management efforts.

KEYWORDS: mangrove, UAV, individual tree detection, LiDAR, kernel, window size

CITATION: Muhammad Rizki Nandika, Jeverson Renyaan, Bayu Prayudha, La Ode Alifatri, Herlambang Aulia Rachman, Yaya Ihya Ulumuddin, Turissa Pragunanti Ilyas, Dony Kushardono, Martiwi Diah Setiawati(2025). How Drones And Lidar Help In Counting Mangrove Trees: A Practical Approach. Geography, Environment, Sustainability, 3 (18), 88-98 https://doi.org/10.24057/2071-9388-2025-3958

ACKNOWLEDGEMENTS: The first author contributed to conceptualization, methodology, and writing of the original draft. The second author was responsible for data curation and writing—review and editing. The third author contributed to supervision and writing—review and editing. The fourth author handled data curation and writing—review and editing. The fifth author, sixth author, seventh author, eighth author, and ninth author all contributed to writing—review and editing, with the sixth author also providing supervision.

Conflict of interests: The authors reported no potential conflict of interests.

INTRODUCTION

Mangrove forests are vital coastal ecosystems that provide a wide range of ecological services. They play a crucial role in carbon sequestration, capturing CO₂ and storing it in their biomass and soil (Mumby et al. 2004; Himes-Cornell 2018; Sharifi 2022). These unique ecosystems act as natural barriers against storm surges and coastal erosion, safeguarding coastal communities and infrastructure (Sahu 2015; Giri et al. 2015; Carugati et al. 2018; Giri 2021; Sharifi 2022). Additionally, mangroves support many marine and terrestrial species, making them biodiversity hotspots (Mumby et al. 2004; Sahu 2015; Giri 2021). The role of mangroves in carbon sequestration is particularly vital in

mitigating climate change, as they can store up to four times more carbon per unit area than terrestrial forests.

Monitoring mangrove forests is crucial for their conservation and sustainable management. Traditional methods of counting mangrove trees using ground surveys are labor-intensive, time-consuming, and expensive. These methods often require significant human resources, making them less feasible for large-scale monitoring (Tran et al. 2022). Moreover, the challenging muddy terrain and dangerous wildlife in mangrove ecosystems pose significant risks to researchers, further complicating ground surveys (Rajpar and Zakaria 2014; Saini et al. 2020).

Remote sensing techniques have been widely employed for mangrove monitoring, with satellite imagery

playing a prominent role. Early studies applied terrestrial vegetation indices to mangrove environments (Green et al. 1998), followed by advancements in mangrove classification (Lasalle et al., 2023), development of mangrove-specific indices (Gupta et al. 2018; Diniz et al. 2019; Prayudha et al. 2024), and carbon and biomass estimation from satellite data (Suardana et al. 2023). However, satellitebased methods face limitations in spatial resolution and temporal frequency, constraining their ability to provide detailed information at the scale of individual trees or small clusters. To address these limitations, advancements in remote sensing technologies such as unmanned aerial vehicles (UAVs) have enabled the collection of highresolution imagery and data over targeted areas with greater efficiency and reduced cost (Jones et al. 2020; Tian et al. 2023; Yin et al. 2024). UAVs reduce the need for extensive ground surveys, minimizing risks and logistical challenges (Tamimi and Toth 2024), and provide access to areas difficult to survey on foot.

Among UAV-based technologies, Light Detection and Ranging (LiDAR) is particularly promising for mangrove monitoring. LiDAR employs laser pulses to measure distances between the sensor and objects on the Earth's surface, providing accurate and detailed data on forest structure¹. The system calculates the time taken for the laser pulses to travel to the object and back, using this information to determine the distance with high precision. In mangrove forests, LiDAR can capture detailed images of canopy height, density, and tree distribution, which provide important information regarding the forest's health and composition (Wang et al. 2019; Yin and Wang 2019; Tian et al. 2023; Yin et al. 2024).

LiDAR technology has proven effective in various forest monitoring applications. For instance, studies that specifically utilize LiDAR for mangrove detection have been conducted by various researchers to observe, both to estimate the number of trees and tree height (Kasai et al. 2024; Yin et al. 2024) as well as to calculate mangrove biomass (Fatoyinbo et al. 2018; Qiu et al. 2019; Wang et al. 2019; Wang et al. 2022; Salum et al. 2020; Tian et al. 2021). However, the application of this technology still faces challenges in terms of accuracy and efficiency, particularly in areas with high vegetation density, where under-detection of trees occurs (Yin and Wang 2019).

The Seribu Islands, particularly Pramuka Island, serve as the focus of this study due to their characteristic mangrove plantations. The area consists primarily of a single species, *Rhizophora stylosa*, planted in clusters through community reforestation efforts². This clustered planting results in high tree density, relatively short trees due to nutrient competition, and limited electromagnetic wave penetration, which complicates data acquisition and individual tree discrimination. These conditions provide a unique opportunity to evaluate and optimize the effectiveness of UAV-based LiDAR for individual tree detection in mangrove plantations.

Our research is expected to make a contribution to the conservation and sustainable management of mangrove forests by addressing the challenge of individual tree detection in dense mangrove plantations using UAV LiDAR data. Specifically, we investigate how the smoothing process

and detection window size can affect the accuracy of individual tree detection in this challenging environment. By optimizing these parameters, we seek to enhance detection performance, providing more precise data on mangrove forest structure to support sustainability and environmental management.

MATERIALS AND METHODS

Study Area

The data was collected on Pramuka Island, a small island in the Seribu Islands, Indonesia (Fig. 1). The observed area covers approximately 0.6 ha (6,000 m²), delineated using a rectangular boundary. It consists of a single mangrove species, Rhizophora stylosa, resulting from community planting efforts. The planting technique involved grouping seedlings in clusters, leading to a high-density stand of trees³. As a result, the trees are relatively short due to competition for nutrients. The density of the mangroves also causes low penetration of electromagnetic waves, resulting in limited information availability for ground data. Furthermore, the relatively homogeneous tree height across the plantation makes it difficult to discriminate between individual canopies. These circumstances are interesting to observe, as they provide an opportunity to test the effectiveness of the LiDAR sensor applied in the mangrove plantation community.

Data collection

Aerial imagery was acquired using the DJI M300 RTK UAV equipped with the Zenmuse L1 LiDAR sensor. The LiDAR sensor provides high-resolution point cloud data, which is crucial for accurately mapping and analyzing forest structures. The sensor is capable of a pulse repetition rate of up to 240,000 pulses per second, enabling high-density data recording. Additionally, the sensor integrates data with Global Navigation Satellite System (GNSS) and Inertial Measurement Unit (IMU) systems⁴, providing very high georeferencing accuracy and resulting in highly detailed and accurate data. Table 1 presents the aircraft specifications and sensor used for the acquisition.

The data collection was conducted at 10:00 a.m. local time under clear sky conditions (minimal cloud cover) with a flying altitude of 80 meters. This acquisition process resulted in a total of 339,316 points, providing sufficient detail to capture the structural complexity of the mangrove canopy. Details of the flight settings are provided in Table 2.

Ground truth data were collected through a 10m² transect, encompassing measurements of tree density (including trees, saplings, and seedlings), diameter at breast height (DBH), average tree height, substrate type, and mangrove species composition. GPS was used solely to mark the transect location without recording the exact coordinates of individual trees. This limitation hindered the direct validation of LiDAR data. However, the ground truth data were utilized to estimate tree density and average height as a reference for evaluating the accuracy of individual tree detection (ITD) from the Canopy Height Model (CHM).

¹Codex Y. (2023). Predicting Species Distributions using High-Resolution Remote Sensing Data: A Comprehensive Review and Assessment. Available at: https://codex.yubetsu.com/article/c004a755544b427a942af6ed2580f3f7 [Accessed 10 January 2025]

²Kementerian Lingkungan Hidup dan Kehutanan (KLHK) (2023). Penanaman mangrove dengan sistem rumpun berjarak di Kepulauan Seribu. Available at: https://itjen.menlhk.go.id/berita/penanaman-mangrove-dengan-sistem-rumpun-berjarak-di-kepulauan-seribu [Accessed 10 January 2025]

³Kementerian Lingkungan Hidup dan Kehutanan (KLHK) (2023). Penanaman mangrove dengan sistem rumpun berjarak di Kepulauan Seribu. Available at: https://itjen.menlhk.go.id/berita/penanaman-mangrove-dengan-sistem-rumpun-berjarak-di-kepulauan-seribu [Accessed 10 January 2025].

⁴DJI (2024). Zenmuse L1 specifications. Available at: https://enterprise.dji.com/zenmuse-l1/specs [Accessed: 6 August 2024].

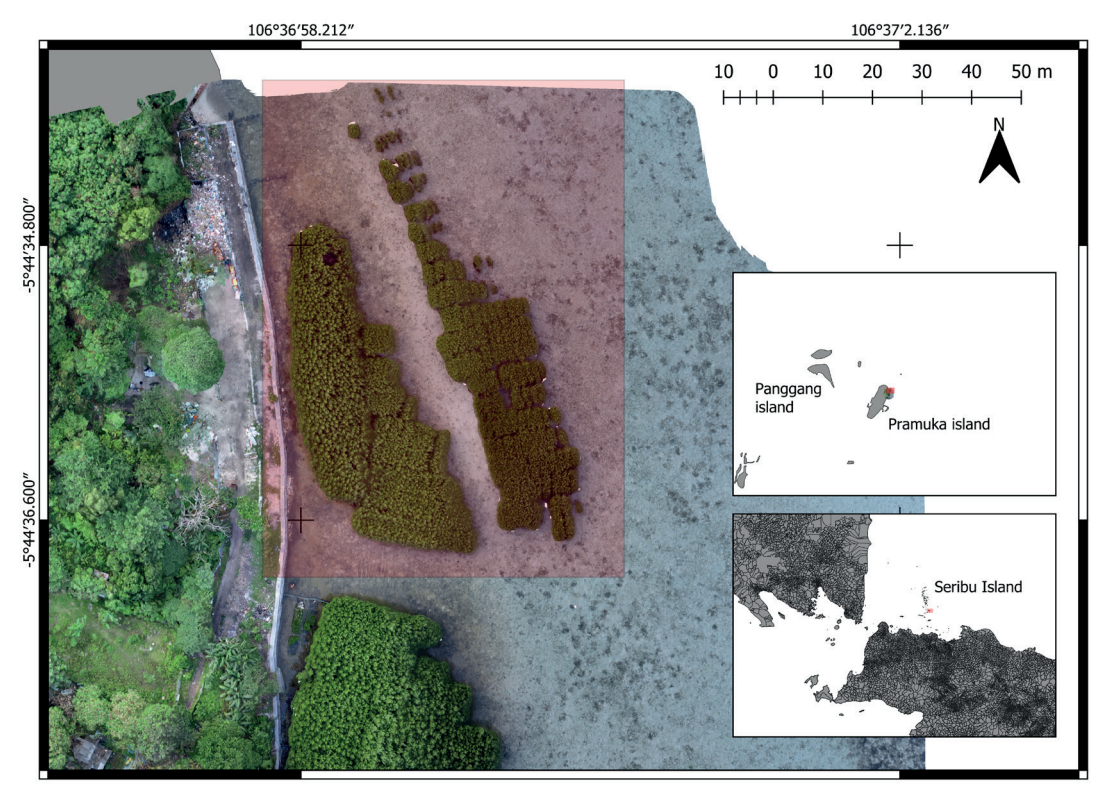


Fig. 1. The study site is located on Pramuka Island. The red box indicates the selected area for this study

Table 1. Aircraft and sensor specifications¹

DJI M300 RTK (Aircraft)	DJI Zenmuse L1 (Camera)				
RTK Positioning Accuracy RTK enabled and fixed: 1 cm + 1 ppm (horizontal) 1.5 cm + 1 ppm (vertical)	Point Rate Single return: 2,400,000 pts/s Multiple returns: 480,000 pts/s System Accuracy Horizontal: 10 cm @ 50 m Vertical: 5 cm @ 50 cm				
Hovering Accuracy (P-mode with GPS) Vertical: ±0.1 m (Vision system enabled) ±0.5 m (GPS enabled) ±0.1 m (RTK enabled) Horizontal: ±0.3 m (Vision system enabled) ±1.5 m (GPS enabled) ±0.1 m (RTK enabled)					
Operating Frequency 2.4000 - 2.4835 GHz 5.725 - 5.850 GHz	Field of View (FOV) Repetitive line scan: 70.4° × 4.5° Non-repetitive line scan: 70.4° × 77.2°				
Max Wind Resistance 12 m/s	Scan Modes Repetitive line scan mode Non-repetitive petal scan mode				
GNSS GPS + GLONASS + BeiDou + Galileo	Maximum Return Supported: 3 Ranging Accuracy: 3 cm @ 100 m				

Data pre-processing

Fig. 2 illustrates the entire process conducted in this study. The captured LiDAR data was initially processed using WebODM, an open-source photogrammetry and 3D reconstruction tool, to generate the 3D point cloud data (LAS file). Processing began with the lidR package (Roussel and Auty 2024) in an R environment⁵.

The LAS file was first converted into a Digital Surface Model (DSM) using the Point-to-Raster (P2R) tool. This step involves transforming the LiDAR points into a 2D raster grid, where each cell (with a pixel size of 0.1 meter) represents

the maximum elevation from the points within the cell. The resulting DSM captures the elevation, both terrain and all above-ground objects, such as vegetation and structures.

To generate a Digital Terrain Model (DTM) a more detailed workflow was applied. The original point cloud was then classified, separating bare earth from vegetation and other non-ground features. The ground-classified points were then interpolated using the Inverse Distance Weighting (IDW) method. This interpolation imparts more weight to nearby ground points, ensuring a smooth and accurate terrain surface (Mohan et al. 2021).

⁵R Core Team (2024). R: A language and environment for statistical computing. R Foundation for Statistical Computing, Vienna, Austria. Available at: https://www.R-project.org/. [Accessed: 10 August 2024]

Table 2. General flight setting

Parameters	Setting
Fly height	80 m
Drone speed (while recording)	8 m/s
Side overlap	50%

Following this, the CHM was produced by normalizing DSM with DTM, specifically by subtracting the DSM with DTM (Pertille et al. 2024). This process removes the ground elevation from the DSM, leaving only the height of vegetation or other objects above the ground. Once the basic data was prepared, the next step was to detect individual trees.

Individual tree detection

Filtering treatment

In tree detection using CHM data, the process typically involves an initial smoothing stage to reduce noise and minor irrelevant variations in the canopy height data. This reduction in noise results in more representative and accurate peak detection. Smoothing also clarifies treetops by diminishing minor variations, making the highest points that represent the treetops more prominent and distinct. Additionally, smoothing helps eliminate minor anomalies or outliers that may not be part of the tree structure, ensuring that irrelevant data does not disrupt peak detection (Pertille et al. 2024).

In this study, the Gaussian method was applied as a filtering treatment. The application of Gaussian filtering plays a crucial role in refining the CHM and improving the accuracy of individual tree detection. In this study, we tested a range of square-shaped kernel sizes, including unfiltered CHM and 3×3 , 5×5 , 9×9 , 11×11 , and 21×21 kernel sizes. These filters were used to smooth the CHM and remove noise while retaining critical information for detecting individual mangrove trees (Pertille et al. 2024).

Local maxima method and window size treatment

A relatively straightforward method for detecting individual trees on the LiDAR-derived CHM is the Local Maxima (LM) algorithm. The LM method assumes that local height maxima in the CHM represent treetops (Korpela 2006). This method is relatively simple and uses two main parameters: a smoothing parameter, often referred to as the smoothing window size (SWS), and a fixed window size (FWS) for tree detection (Silva et al. 2016). As the FWS increases, the number of detected trees decreases (Mohan et al. 2017). Applying smoothing filters helps eliminate invalid local maxima caused by significant, spreading tree branches, thereby reducing the number of detected local maxima and improving the algorithm's accuracy (Lindberg and Hollaus 2012).

In this study, we tested various combinations of CHM smoothing kernel sizes and LMF window sizes to evaluate their effect on individual tree detection performance. The smoothing kernel sizes included unfiltered, 3×3 , 5×5 , 9×9 , 11×11 , and 21×21 , each applied with LMF window sizes of 0.5 m, 1 m, and 3 m.

F-score calculation

To evaluate the accuracy of individual tree detection, this study employed the F-score (F1) as a performance metric. The F-score is the harmonic mean of precision and recall, which balances the trade-off between detecting true positives (TP) while minimizing false positives (FP) and false negatives (FN) (Power 2011). This metric has also been widely adopted in similar studies related to UAV-based tree detection (Mohan et al. 2017; Ahmadi et al. 2022)

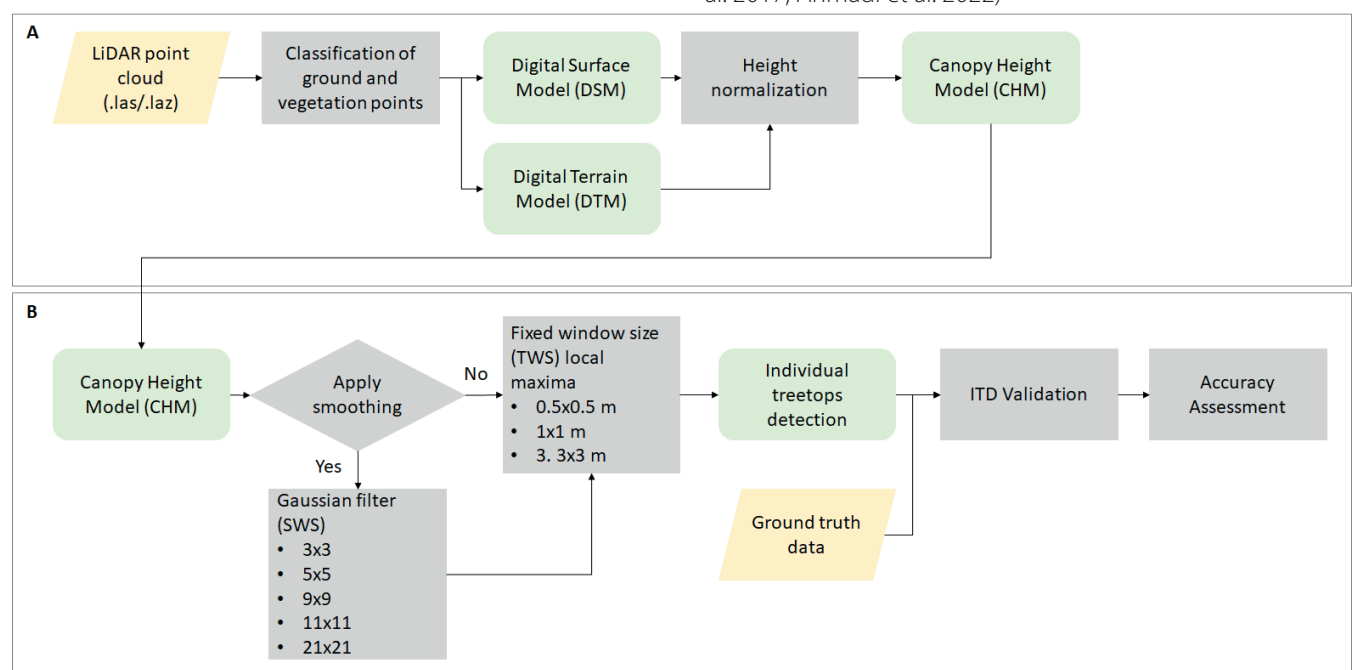


Fig. 2. Workflow of LiDAR data pre-processing and local-maxima-based individual tree detection (ITD) methodology. (A) LiDAR data pre-processing steps include filtering, normalization, point classification, noise removal, and data fusion to prepare the data for analysis. (B) Local-maxima-based individual tree detection involves the generation of the Canopy Height Model (CHM), followed by the detection of local maxima to identify tree tops and subsequent clustering to delineate individual trees

Given that UAV-based tree detection can result in both overestimation (FP > 0) and underestimation (FN < 0), this metric provides a comprehensive measure of detection effectiveness. The precision (P), recall (R), and F-score (F1) were calculated using the following Eqs. 1-3 (Power 2011):

$$Precision = \frac{TP}{TP + FP} \tag{1}$$

$$Recall = \frac{TP}{TP + FN} \tag{2}$$

$$F1 - score = 2x \frac{Precision \times Recall}{Precision + Recall}$$
(3)

True positives (TP) represent the number of trees detected by the UAV that match the expected tree count in the field. False negatives (FN) refer to trees that were present in the field but were not detected by the UAV. On the other hand, false positives (FP) indicate trees that were counted by the UAV but do not correspond to trees in the field. These definitions help evaluate the accuracy of the UAV-based tree detection system by assessing how well the detected trees align with the actual tree count in the field. Since ground-truth data on tree positions were unavailable, TP, FP, and FN were estimated based on the total number of trees recorded in the field rather than a tree-to-tree spatial validation. This is a clear limitation of the study, as the lack of spatial correspondence between UAV-detected trees and field-observed trees prevents the accurate matching of individual trees. As an alternative, TP, FP, and FN were approximated using total tree counts per plot. A detection was considered a true positive if it occurred within the plot area and the total number of UAV-detected trees did not exceed the field count. In underestimation cases (UAV count < field count), all detected trees were assumed to be true positives, and FP was set to zero. In contrast, if the UAV count exceeded the field count, the surplus detections were considered false positives. While this method does not allow spatially explicit matching between detected and actual trees, it does not replace precise spatial validation and should be interpreted accordingly.

RESULT

The UAV-acquired imagery was precisely cropped at the observation site to obtain more accurate and reliable data. This cropping process was designed to exclude non-target objects such as buildings, water bodies, or non-mangrove vegetation. By eliminating these elements, the precision of the CHM information was enhanced, resulting in cleaner data with minimal external interference. This process ensures that the analytical results have a high level of accuracy and are relatively free from errors, thereby improving the reliability of the data for this study. Fig. 3

shows the results of the 3D point cloud cropped specifically for the selected area.

CHM Normalization

The DSM showed elevation values ranging from 25.6 to 34.10 meters, capturing both ground and above-ground features such as vegetation and structures. In contrast, the DTM exhibited a narrower elevation range of 25.6 to 26.853 meters, indicating minimal elevation difference across the terrain. This relatively flat ground surface is consistent with typical mangrove habitats. However, in several areas, the DTM failed to fully represent the terrain due to limited ground returns. These gaps are not visually apparent in DTM figures but should be taken into account when interpreting the CHM result. Despite the limitation, the CHM was successfully generated by normalizing DSM with DTM (Gomroki et al. 2017), producing a height range from -0.24 to 7.59 meters. Fig. 4 illustrates the difference in height patterns before and after normalization.

Effects of Kernel and Window Size on Tree Detection Accuracy

The unfiltered CHM produced a noisy image with numerous local maxima that did not correspond to actual tree tops, primarily due to variations in the canopy structure, such as large branches or small gaps. This excessive noise compromised tree detection accuracy using the Local Maxima (LM) algorithm (Lisiewicz et al. 2022). In contrast, the 3×3 kernel applied a light smoothing filter, effectively reducing noise while preserving important canopy details. It eliminated minor irregularities and allowed for more accurate tree detection, especially in dense and uniform canopy structures. Visually, the CHM with a 3×3 kernel would show a more controlled and smoother image, with less color variation between areas, preserving the essential tree structures while softening the noise (Fig. 5).

As the kernel size increased to 5×5, 9×9, 11×11, 21×21, the CHM became progressively smoother. The 5×5 kernel removed additional noise and minor fluctuations, providing a balance between smoothing and preserving canopy details. However, larger kernel sizes like 9×9, 11×11, and 21×21 introduced excessive smoothing, which led to the merging of nearby treetops and a significant underestimation of the number of detected trees. The 21×21 kernel, in particular, overgeneralized the canopy, removing critical details about individual trees and rendering it unsuitable for dense mangrove forests (Tanhuanpaa et al. 2019; Quan et al. 2021).

Various combinations of kernel sizes (unfiltered, 3×3 , 5×5 , 9×9 , 11×11 , 21×21) and Local Maximum Filter (LMF) window sizes (0.5, 1, and 3 meters) were applied to analyze mangrove tree density (Fig. 6). The results indicate that smaller window sizes detect more trees due to their

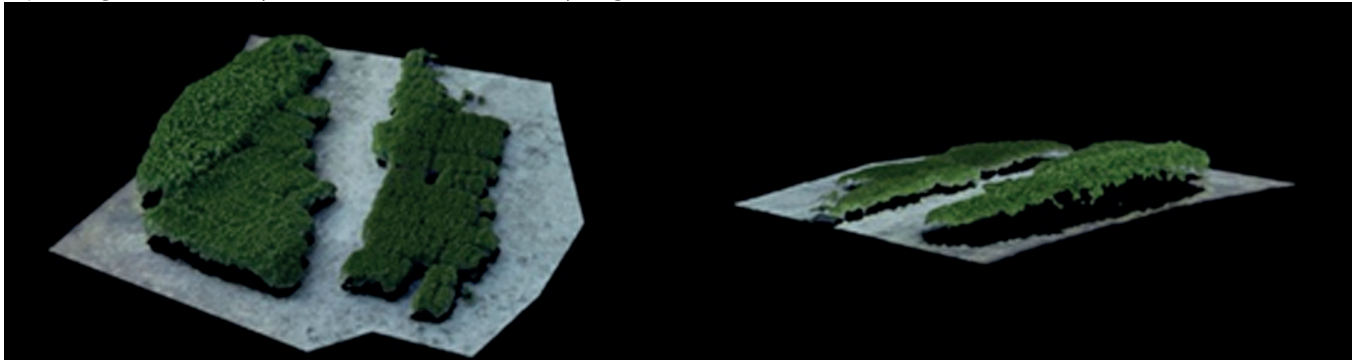


Fig. 3. 3D RGB LiDAR data of mangrove in Pramuka Island

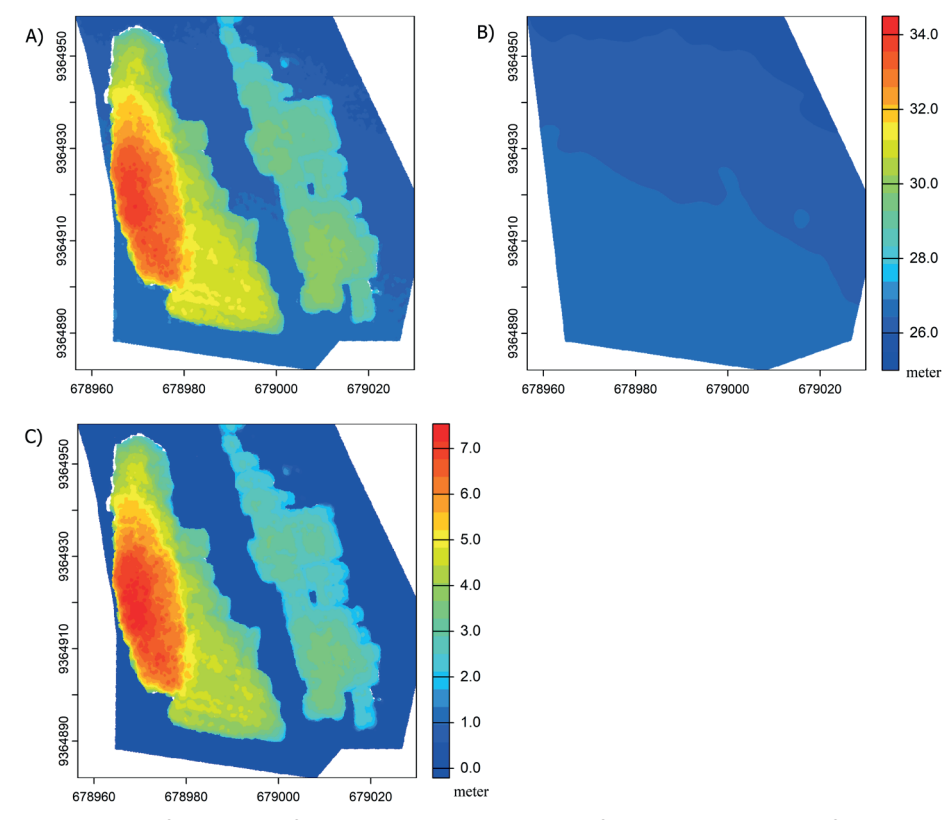


Fig. 4. Visualization of data at different stages: A) Digital Surface Model (DSM) before normalization; B) Digital Terrain Model (DTM); and C) Canopy Height Model (CHM) after normalization – in meter

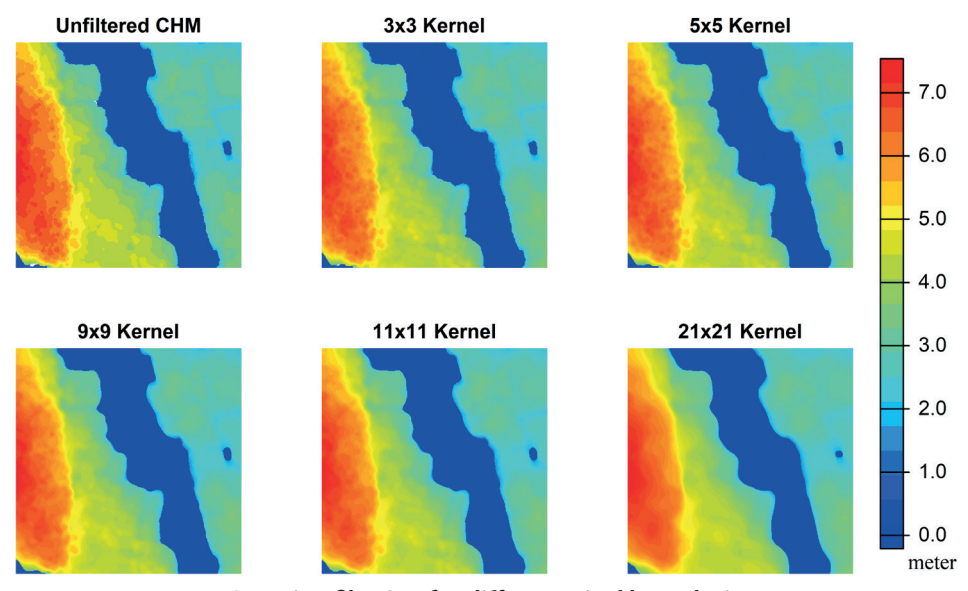


Fig. 5. Gaussian filtering for different pixel kernel - in meter

sensitivity to local variations. However, these findings may lead to overestimation in dense mangrove stands, where the algorithm may misidentify non-tree objects as treetops (Yan et al. 2024).

On the other hand, larger kernels and window sizes smooth out local variations, producing more refined estimates by reducing over-detection errors. While such practices may reduce the risk of excessive detection errors, using large kernels and window sizes can obscure important local details and lead to underestimating the number of trees (Balsi et al. 2018).

Given the limited field data obtained specifically from Pramuka Island, we attempted to broaden the scope of analysis by incorporating field data from several observation points on other islands within the Seribu Islands (Table 3). This approach is feasible due to the homogeneity of mangrove ecosystems across the Seribu Islands, where most of the mangroves are cultivated, predominantly consisting of *Rhizophora mucronata* and *Rhizophora stylosa*, and planted using a clustered spacing system⁶. This uniformity results in relatively similar structural patterns across the mangrove areas in the region.

The detection results show that using a window size of 0.5 meters, supported by kernels 3×3, 5×5, and 9×9, provides more accurate detection of mangroves, aligning with the average number of tree-phase mangroves found in the Seribu Islands (Fig. 7). This smaller window size is particularly effective in dense mangrove conditions, where

⁶Kementerian Lingkungan Hidup dan Kehutanan (KLHK) (2023). Penanaman mangrove dengan sistem rumpun berjarak di Kepulauan Seribu. Available at: https://itjen.menlhk.go.id/berita/penanaman-mangrove-dengan-sistem-rumpun-berjarak-di-kepulauan-seribu [Accessed 10 January 2025].

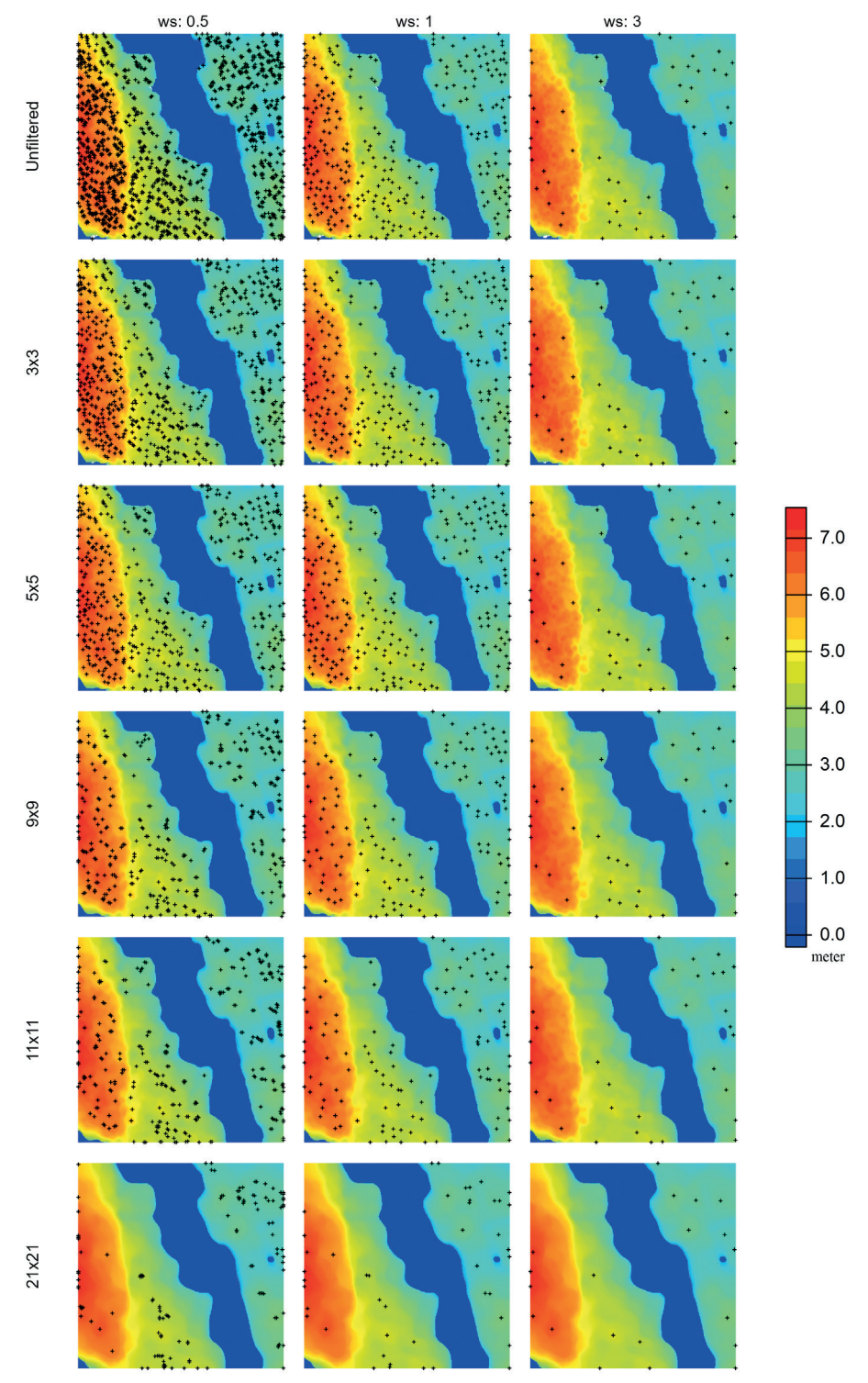


Fig. 6. Tree detection using the Local Maxima function with different window sizes for each kernel. In every kernel, a window size of 1 meter provides more detailed and numerous tree point information compared to larger window sizes (3 and 5 meters)

it can detect individual trees more accurately, especially in high-density areas (Kim et al., 2020). In contrast, using larger window sizes, such as 1 and 3 meters, tends to result in underestimates, except for the 1-meter window size combined with the 3×3 kernel, which aligns well with field data. Larger window sizes often lead to over smoothing, which hinders the detection of smaller or hidden trees beneath larger canopies (Balsi et al., 2018). Additionally, unfiltered data combined with a 0.5×0.5 meter window size leads to an overestimate, as unfiltered data does not distinguish well between mangrove trees and other objects, resulting in more trees being detected than are actually present. Despite these configurations yielding better results, all detection outcomes (except for

the unfiltered configuration with kernel 0.5×0.5) are still underestimated compared to mangrove plots at specific locations on Pramuka Island. This highlights that LiDAR still struggles to distinguish individual mangrove trees with homogeneous heights, as this condition creates a bias where crowns overlap, making it difficult to clearly define the boundaries between individual trees (Galvincio & Popescu, 2016).

The analysis revealed that mangrove plots that had reached the tree growth stage—where tree-stage mangroves are the only ones detectable via drone imagery, unlike saplings and seedlings, which are often obscured by the tree canopy—contained between 19 and 63 individuals per 100 m². Additionally, the areas observed by drone

Table 3. Field Data of 10 mangrove plot points in the Seribu Islands, including substrate type, trees, saplings, and seedlings measurements

Plot Code	Lat (°)	Lon (°)	Substrate Type	Trees (ind./plot)	Saplings (ind./plot)	Seedlings (ind./plot)	
Panggang 1	-5.74243	106.6041	Sandy mud	57	56	0	
Panggang 2	-5.74196	106.6039	Sandy mud 21 96		4		
Kelapa 1	-5.64895	106.5671	Sandy mud	0	390	0	
Kelapa 2	-5.6568	106.5639	Sandy mud	25	216	0	
Kelapa-Harapan	-5.65228	106.5743	Muddy sand	9	229	0	
Harapan	-5.65379	106.5808	Muddy sand	9	243	0	
Pari	-5.85288	106.6208	Sandy mud	43	4	10	
Pramuka 1	-5.74391	106.6162	Sandy mud	63	65	2	
Pramuka 2	-5.74527	106.615	Sandy mud	61	66	0	
Pramuka 3	-5.74874	106.6116	Sandy mud	6	209	0	

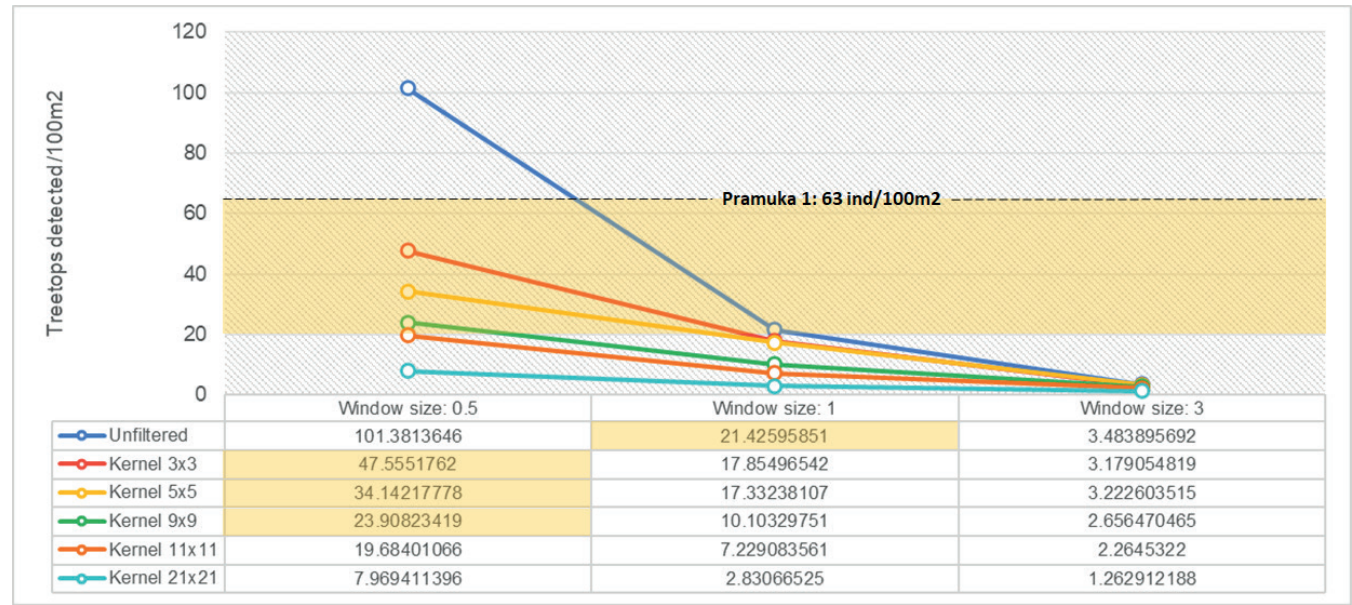


Fig. 7. Treetop Detection Density (ind./100m²) Across Different Kernel Sizes and Window Sizes Compared to Field Data (Pramuka 1: 63 ind/100m²)

specifically consisted of tree-stage mangroves, as this is the only stage where accurate observation and counting from aerial imagery are feasible, given the limitations of drone detection for saplings and seedlings (Hsu et al., 2020; Bakar et al., 2024).

Conversely, plots containing mangroves at the seedling stage exhibited much higher densities, with over 200 individuals per 100 m². This is due to the clustered spacing planting method⁷, which supports mangrove growth up to the seedling stage.

Evaluation of F-score in UAV-based tree detection

This study applied various combinations of smoothing kernel sizes and local maxima filtering (LMF) window sizes to optimize individual tree detection from CHM (Table 4). The F-score was calculated for each combination to determine which method yielded the best balance between minimizing false positives (FP) and maximizing true positives (TP) while reducing false negatives (FN).

A higher F-score indicates that the method correctly identifies trees and minimizes errors.

The highest F-score was achieved using the Kernel 3×3/WS 0.5 method (F1-score = 0.854), which provided the best trade-off between precision and recall. This method detected 47 of the 63 trees recorded in the field, resulting in a relatively high recall (0.746). This combination effectively minimized FN, making it the most balanced approach in the study. In contrast, methods with larger smoothing kernels and window sizes (e.g., Kernel 9×9/WS 3, Kernel 21×21/WS 3) had extremely low recall (0.031–0.047), leading to F-scores below 0.1. These methods failed to detect a significant portion of the trees due to excessive smoothing, which merged adjacent treetops and resulted in severe under detection.

DISCUSSION

This study aimed to detect and analyze individual mangrove trees using LiDAR-derived Canopy Height

⁷Kementerian Lingkungan Hidup dan Kehutanan (KLHK) (2023). Penanaman mangrove dengan sistem rumpun berjarak di Kepulauan Seribu. Available at: https://itjen.menlhk.go.id/berita/penanaman-mangrove-dengan-sistem-rumpun-berjarak-di-kepulauan-seribu [Accessed 10 January 2025].

Table 4. F1-score for all of the configuration

				•			
Method	UAV Count	TP	FP	FN	Precision	Recall	F1-Score
Kernel 3×3/WS 0.5	47	47	0	16	1	0.746	0.8545
Unfiltered/WS 0.5	101	63	38	0	0.6238	1	0.7683
Kernel 5×5/WS 0.5	34	34	0	29	1	0.54	0.701
Kernel 9x9/WS 0.5	23	23	0	40	1	0.365	0.5349
Unfiltered/WS 1	21	21	0	42	1	0.333	0.5
Kernel 11×11/WS 0.5	19	19	0	44	1	0.302	0.4634
Kernel 3×3/WS 1	17	17	0	46	1	0.27	0.425
Kernel 5×5/WS 1	17	17	0	46	1	0.27	0.425
Kernel 9×9/WS 1	10	10	0	53	1	0.159	0.2739
Kernel 11×11/WS 1	7	7	0	56	1	0.111	0.2
Kernel 21×21/WS 0.5	7	7	0	56	1	0.111	0.2
Unfiltered/WS 3	3	3	0	60	1	0.048	0.0909
Kernel 3×3/WS 3	3	3	0	60	1	0.048	0.0909
Kernel 5×5/WS 3	3	3	0	60	1	0.048	0.0909
Kernel 9×9/WS 3	2	2	0	61	1	0.032	0.0615
Kernel 11×11/WS 3	2	2	0	61	1	0.032	0.0615
Kernel 21×21/WS 1	2	2	0	61	1	0.032	0.0615
Kernel 21×21/WS 3	1	1	0	62	1	0.016	0.0313

Model (CHM) in a dense mangrove forest. The challenge of accurately extracting tree heights and positions in such complex environments is well-known due to structural variability and occlusions in the canopy. LiDAR data processing, including Digital Terrain Model (DTM) generation and smoothing of CHM data, plays a critical role in minimizing errors and improving tree detection accuracy.

One significant limitation encountered was the dense mangrove canopy, which likely obstructed the LiDAR sensor's ability to penetrate through to the ground, resulting in interpolation gaps and uneven terrain surfaces (Wannasiri et al. 2013; Balsi et al. 2018; Yin & Wang 2019; Li et al. 2023; Wijaya et al. 2023). This limited ground return coverage can affect the accuracy and reliability of the DTM, which in turn impacts the derived CHM and its interpretation. Although these interpolation gaps are not visually apparent in the DTM figures, they may lead to underestimation or spatial inconsistency in canopy height measurements. Future studies could consider integrating additional ground-based surveys or complementary remote sensing data to improve terrain representation in dense mangrove environments.

The unfiltered CHM's noise was mainly caused by structural variations in the canopy, such as large branches or small gaps, leading to numerous false local maxima and reduced tree detection accuracy with the Local Maxima algorithm (Lisiewicz et al. 2022). Applying a 3×3 Gaussian kernel offered light smoothing, which effectively reduced noise while preserving essential canopy features, thus improving detection in dense mangrove canopies.

Increasing kernel sizes progressively smoothed the CHM but introduced trade-offs. The 5×5 kernel

balanced noise reduction and detail preservation, while larger kernels (9×9 and above) excessively smoothed the canopy, causing merging of adjacent treetops and underestimation of tree counts. The 21×21 kernel was particularly overgeneralizing, losing vital individual tree information and making it unsuitable for dense mangrove forests. This excessive smoothing reduces color and height variation, impairing the ability to distinguish individual trees in complex environments (Tanhuanpaa et al. 2019; Quan et al. 2021).

Choosing an appropriate kernel size is therefore critical to optimize the balance between noise suppression and canopy detail preservation in mangrove tree detection. These findings indicate a significant trade-off in selecting kernel and window sizes for optimal tree detection. Smaller LMF window sizes, while sensitive to minor variations, may not be appropriate in dense mangrove conditions, as they increase the likelihood of detecting false positives. Conversely, larger kernels and window sizes improve robustness against noise but risk underestimating true tree counts by merging individual tree signals and suppressing fine-scale canopy variation. While the 3x3 kernel and 0.5-meter window size yielded the best results in this study, this outcome should be interpreted with caution. The performance of these parameters is strongly influenced by the CHM pixel resolution (10 cm) and the relatively high density and structural uniformity of mangrove trees in the Seribu Islands. Parameter effectiveness may vary in different contexts, such as areas with lower tree density, heterogeneous canopy structures, or different CHM resolutions. Therefore, selecting kernel and window sizes should be context-specific, reflecting both the spatial resolution and vegetation characteristics of the study area. Due to the lack of spatial ground-truth data containing exact tree positions, the F-score calculation in this study was based solely on the total number of detected trees rather than a one-to-one comparison of detected and actual trees. As a result, precision remained at 1.0 for all methods except Unfiltered/WS 0.5 since false positives (FP) were assumed to be zero in all underestimated cases. This means that every detected tree was considered correct despite the potential presence of undetected trees (false negatives, FN). Consequently, although precision appears perfect, recall remains significantly lower in most cases, leading to low F-scores for many methods. This highlights the limitations of relying solely on precision when evaluating detection performance in an underestimation scenario.

CONCLUSION

This study successfully demonstrated the potential of UAV LiDAR technology in monitoring mangrove forests. The optimum configuration, using a 3×3 kernel with a 0.5 meter window size, achieved the best balance between detection accuracy and noise reduction. These findings highlight that parameter tuning is critical to optimize

detection performance, especially in complex and dense vegetation environments like mangroves. Despite its potential, LiDAR's limited ability to penetrate dense vegetation is a significant challenge. Thick foliage and branches obstruct the sensor's signal, making it difficult for the signal to reach the ground, which in turn limits the availability of accurate ground elevation. The selection of kernel and window sizes plays a key role in tree detection accuracy. Smaller window sizes tend to capture more trees by focusing on finer local details. However, smaller windows might lead to overcounting trees or misidentifying nontree objects as treetops in areas with dense vegetation. On the other hand, using larger kernels and window sizes can reduce the level of detail and smooth the data, which may lead to a loss of local variations and a decrease in the accuracy of tree detection.

Future research should to refine measurement parameters to enhance tree detection in dense mangrove forests. It is also critical to develop more advanced algorithms that consider the specific conditions of the study area. By integrating LiDAR data with other monitoring methods, the overall quality and accuracy of the data can be improved, further supporting the conservation and management of mangrove forests.

REFERENCES

Ahmadi S. A., Ghorbanian A., Golparvar F., Mohammadzadeh A. and Jamali S. (2022). Individual tree detection from unmanned aerial vehicle (UAV) derived point cloud data in a mixed broadleaf forest using hierarchical graph approach. European Journal of Remote Sensing, 55(1), pp.520-539, DOI: 10.1080/22797254.2022.2129095

Bakar N.A.A., Jaafar W.S.W.M., Maulud K.N.A., Kamarulzaman A.M.M., Saad S.N.M., Mohan M. (2024). Monitoring mangrove-based blue carbon ecosystems using UAVs: a review. Geocarto International, 39:1, 2405123, DOI: 10.1080/10106049.2024.2405123.

Balsi M., Esposito S., Fallavollita P. and Nardinocchi C. (2018). Single-tree detection in high-density LiDAR data from UAV-based survey. European Journal of Remote Sensing, 51(1), pp.679-692, DOI: 10.1080/22797254.2018.1474722.

Carugati L., Gatto B., Rastelli E., Lo Martire M., Coral C., Greco S. and Danovaro R. (2018). Impact of mangrove forests degradation on biodiversity and ecosystem functioning. Scientific Reports, 8, 13298, DOI: 10.1038/s41598-018-31683-0.

Diniz C., Cortinhas L., Nerino G., Rodrigues J., Sadeck L., Adami M. and Souza-Filho P.W.M. (2019). Brazilian mangrove status: Three decades of satellite data analysis. Remote Sensing, 11(7), p.808, DOI: 10.3390/rs11070808

Fatoyinbo T., Feliciano E.A., Lagomasino D., Lee S.K. and Trettin C. (2018). Estimating mangrove aboveground biomass from airborne LiDAR data: a case study from the Zambezi River delta. Environmental Research Letters, 13(2), p.025012, DOI: 10.1088/1748-9326/aa9f03.

Galvincio J.D., and Popescu S.C. (2016). Measuring individual tree height and crown diameter for mangrove trees with airborne LiDAR data. International Journal of Advanced Engineering, Management & Science, 2(5), pp.431-443.

Giri C. (2021). Recent advancement in mangrove forests mapping and monitoring of the world using earth observation satellite data. Remote Sensing, 13(4), p.563, DOI: 10.3390/rs13040563.

Giri C., Long J., Abbas S., Murali R.M., Qamer F.M., Pengra B. and Thau D. (2015). Distribution and dynamics of mangrove forests of South Asia. Journal of Environmental Management, 148, pp.101-111, DOI: 10.1016/j.jenvman.2014.01.020.

Glotfelty J.E. (1999). Automatic selection of optimal window size and shape for texture analysis. West Virginia University.

Gomroki M., Jafari M., Sadeghian, S. and Azizi Z. (2017). Application of intelligent interpolation methods for DTM generation of forest areas based on LiDAR data. PFG–Journal of Photogrammetry, Remote Sensing and Geoinformation Science, 85, pp.227-241, DOI: 10.1007/s41064-017-0025-0.

Green E.P., Clark C.D., Mumby P.J., Edwards A.J. and Ellis A.C. (1998). Remote sensing techniques for mangrove mapping. International journal of remote sensing, 19(5), pp.935-956, DOI: 10.1080/014311698215801.

Gupta K., Mukhopadhyay A., Giri S., Chanda A., Majumdar S.D., Samanta S., Mitra D., Samal R.N., Pattnaik A.K. and Hazra S., 2018. An index for discrimination of mangroves from non-mangroves using LANDSAT 8 OLI imagery. MethodsX, 5, pp.1129-1139, DOI: 10.1016/j.mex.2018.09.011 Himes-Cornell A., Pendleton L. and Atiyah P. (2018). Valuing ecosystem services from blue forests: A systematic review of the valuation of salt marshes, sea grass beds and mangrove forests. Ecosystem Services, 30, pp.36-48, DOI: 10.1016/j.ecoser.2018.01.006.

Hsu A.J., Kumagai J., Favoretto F., Dorian J., Martinez B.G., Aburto-Oropeza O. (2020). Driven by drones: Improving mangrove extent maps using high-resolution remote sensing. Remote Sensing, 12(23), p.3986, DOI: 10.3390/rs12233986.

Jones A.R., Raja Segaran R., Clarke K.D., Waycott M., Goh W.S. and Gillanders B.M. (2020). Estimating mangrove tree biomass and carbon content: a comparison of forest inventory techniques and drone imagery. Frontiers in Marine Science, 6, p.784, DOI: 10.3389/fmars.2019.00784.

Kasai K., Yanagisawa H. and Goto K. (2024). Quantification of the spatial distribution of individual mangrove tree species derived from LiDAR point clouds. Progress in Earth and Planetary Science, 11(1), p.2, DOI: 10.1186/s40645-024-00626-x.

Kim J., Popescu S.C., Lopez R.R., Ben Wu X., Silvy N.J. (2020). Vegetation mapping of No Name Key, Florida using lidar and multispectral remote sensing. International Journal of Remote Sensing, 41(24), pp.9469-9506, DOI: 10.1080/01431161.2020.1800125.

Korpela I. (2006). Geometrically accurate time series of archived aerial images and airborne lidar data in a forest environment. Silva Fennica, 40(1), p.109, DOI: 10.14214/sf.355.

Lassalle G., Ferreira M.P., La Rosa L.E.C., Scafutto R.D.P.M. and de Souza Filho C.R. (2023). Advances in multi-and hyperspectral remote sensing of mangrove species: A synthesis and study case on airborne and multisource spaceborne imagery. ISPRS Journal of Photogrammetry and Remote Sensing, 195, pp.298-312, DOI: 10.1016/j.isprsjprs.2022.12.003.

Li Q., Wong F.K.K., Fung T., Brown L.A. and Dash J. (2023). Assessment of active LiDAR data and passive optical imagery for double-layered mangrove leaf area index estimation: a case study in Mai Po, Hong Kong. Remote Sensing, 15(10), p.2551, DOI: 10.3390/rs15102551.

Lindberg E. and Hollaus M. (2012). Comparison of methods for estimation of stem volume, stem number and basal area from airborne laser scanning data in a hemi-boreal forest. Remote Sensing, 4(4), pp.1004-1023, DOI: 10.3390/rs4041004.

Lisiewicz M., Kamin'ska A. and Steren'czak K. (2022). Recognition of specified errors of Individual Tree Detection methods based on Canopy Height Model. Remote Sensing Applications: Society and Environment, 25, p.100690, DOI: 10.1016/j.rsase.2021.100690.

Mohan M., Silva C.A., Klauberg C., Jat P., Catts G., Cardil A., Hudak A.T. and Dia M. (2017). Individual tree detection from unmanned aerial vehicle (UAV) derived canopy height model in an open canopy mixed conifer forest. Forests, 8(9), p.340, DOI: 10.3390/f8090340.

Mohan M., Leite R.V., Broadbent E.N., Wan Mohd Jaafar W.S., Srinivasan S., Bajaj S., Dalla Corte A.P., do Amaral C.H., Gopan G., Saad S.N.M. and Muhmad Kamarulzaman A.M. (2021). Individual tree detection using UAV-lidar and UAV-SfM data: A tutorial for beginners. Open Geosciences, 13(1), pp.1028-1039, DOI: 10.1515/geo-2020-0290.

Mumby P.J., Edwards A.J., Ernesto Arias-Gonz´alez J., Lindeman K.C., Blackwell P.G., Gall A., Gorczynska M.I., Harborne A.R., Pescod C.L., Renken H. and Wabnitz, C.C. (2004). Mangroves enhance the biomass of coral reef fish communities in the Caribbean. Nature, 427(6974), pp.533-536, DOI: 10.1038/nature02286.

Pertille C.T., Gomes K.M.A., Veras H.F.P., Mohan M., Sanquetta C.R., Behling A. and Dalla Corte A.P. (2024). Effects of flight and smoothing parameters of number of trees with aerial imagery in a native Brazilian atlantic forest remnant. CERNE, 30(1), DOI:10.1590/01047760202330013338. Powers D.M. (2011). Evaluation: from precision, recall and F-measure to ROC, informedness, markedness and correlation.

Prayudha B., Ulumuddin Y.I., Siregar V., Agus S.B., Prasetyo L.B., Avianto P. and Ramadhani M.R. (2024). Enhanced mangrove index: A spectral index for discrimination understorey, nypa, and mangrove trees. MethodsX, 12, p.102778, DOI: 10.1016/j.mex.2024.102778.

Qiu P., Wang D., Zou X., Yang X., Xie G., Xu S. and Zhong Z. (2019). Finer resolution estimation and mapping of mangrove biomass using UAV LiDAR and worldview-2 data. Forests, 10(10), p.871, DOI: 10.3390/f10100871.

Quan Y., Li M. and Wang B. (2021). Comparison and evaluation of different pit-filling methods for generating high-resolution canopy height model using UAV laser scanning data. Remote Sensing, 13, p.2239, DOI: 10.3390/rs13122239.

Rajpar M.N. and Zakaria M. (2014). Mangrove fauna of Asia. In: Mangrove ecosystems of Asia: Status, challenges and management strategies, pp.153-197, DOI: 10.1007/978-1-4614-8582-7 8.

Roussel J.R., Auty D., Coops N.C., Tompalski P., Goodbody T.R., Meador A.S., Bourdon J.F., De Boissieu F. and Achim A. (2020). lidR: An R package for analysis of Airborne Laser Scanning (ALS) data. Remote Sensing of Environment, 251, p.112061, DOI: 10.1016/j.rse.2020.112061.

Sahu S.C., Suresh H.S., Murthy I.K. and Ravindranath N.H. (2015). Mangrove area assessment in India: Implications of loss of mangroves. J. Earth Sci. Clim. Change, 6(5), p.280, DOI: 10.4172/2157-7617.1000280.

Saini O., Bhardwaj A. and Chatterjee R.S. (2020), November. The Potential of L-Band UAVSAR Data for the Extraction of Mangrove Land Cover Using Entropy and Anisotropy Based Classification. In Proceedings, 46(1), p.21, DOI: 10.3390/ecea-5-06673.

Salum R.B., Souza-Filho P.W.M., Simard M., Silva C.A., Fernandes M.E., Cougo M.F., do Nascimento Junior W. and Rogers K. (2020). Improving mangrove above-ground biomass estimates using LiDAR. Estuarine, Coastal and Shelf Science, 236, p.106585, DOI: 10.1016/j.ecss.2020.106585.

Sharifi A., Felegari S. and Tariq A. (2022). Mangrove forests mapping using Sentinel-1 and Sentinel-2 satellite images. Arabian Journal of Geosciences, 15(20), p.1593, DOI: 10.1007/s12517-022-10867-z.

Silva C.A., Hudak A.T., Vierling L.A., Loudermilk E.L., O'Brien J.J., Hiers J.K., Jack S.B., Gonzalez-Benecke C., Lee H., Falkowski M.J. and Khosravipour A. (2016). Imputation of individual longleaf pine (Pinus palustris Mill.) tree attributes from field and LiDAR data. Canadian Journal of Remote Sensing, 42(5), pp.554-573, DOI: 10.1080/07038992.2016.1196582.

Suardana A.M.A.P., Anggraini N., Nandika M.R., Aziz K., As-Syakur A.R., Ulfa A., Wijaya A.D., Prasetio W., Winarso G. and Dewanti R. (2023). Estimation and mapping above-ground mangrove carbon stock using sentinel-2 data derived vegetation indices in Benoa Bay of Bali Province, Indonesia. Forest and Society, 7(1), pp.116-134, DOI: 10.24259/fs.v7i1.22062.

Tamimi R. and Toth C. (2024). Accuracy Assessment of UAV LiDAR Compared to Traditional Total Station for Geospatial Data Collection in Land Surveying Contexts. The International Archives of the Photogrammetry, Remote Sensing and Spatial Information Sciences, 48, pp.421-426, DOI: 10.5194/isprs-archives-XLVIII-2-2024-421-2024, 2024.

Tanhuanpaa T., Yu X., Luoma V., Saarinen N., Raisio J., Hyyppa J., Kumpula T. and Holopainen M. (2019). Effect of canopy structure on the performance of tree mapping methods in urban parks. Urban Forestry & Urban Greening, 44, p.126441, DOI: 10.1016/j.ufug.2019.126441.

Tian Y., Huang H., Zhou G., Zhang Q., Tao J., Zhang Y. and Lin J. (2021). Aboveground mangrove biomass estimation in Beibu Gulf using machine learning and UAV remote sensing. Science of the Total Environment, 781, p.146816, DOI: 10.1016/j.scitotenv.2021.146816.

Tian Y., Huang H., Zhou G., Zhang Q., Xie X., Ou J., Zhang Y., Tao J. and Lin J. (2023). Mangrove biodiversity assessment using UAV LiDAR and hyperspectral data in China's Pinglu canal estuary. Remote Sensing, 15(10), p.2622, DOI: 10.3390/rs15102622.

Tran T.V., Reef R. and Zhu X. (2022). A review of spectral indices for mangrove remote sensing. Remote Sensing, 14(19), p.4868, DOI: 10.3390/rs14194868.

Wannasiri W., Nagai M., Honda K., Santitamnont P. and Miphokasap P. (2013). Extraction of mangrove biophysical parameters using airborne LiDAR. Remote Sensing, 5(4), pp.1787-1808. DOI: 10.3390/rs5041787.

Wang D., Wan B., Qiu P., Zuo Z., Wang R. and Wu X. (2019). Mapping height and aboveground biomass of mangrove forests on Hainan Island using UAV-LiDAR sampling. Remote Sensing, 11(18), p.2156, DOI: 10.3390/rs11182156.

Wang D., Wan B., Qiu P., Tan X. and Zhang Q. (2022). Mapping mangrove species using combined UAV-LiDAR and Sentinel-2 data: Feature selection and point density effects. Advances in Space Research, 69(3), pp.1494-1512, DOI: 10.1016/j.asr.2021.11.020.

Wijaya M.S., Kamal M., Widayani P. and Arjasakusuma S. (2023). Classification of Mangrove Vegetation Structure using Airborne LiDAR in Ratai Bay, Lampung Province, Indonesia. Geoplanning: Journal of Geomatics and Planning, 10(2), pp.123-134, DOI: 10.14710/geoplanning.10.2.123-134.

Yan Y., Lei J., Jin J., Shi S. and Huang Y. (2024). Unmanned Aerial Vehicle Light Detection and Ranging-Based Individual Tree Segmentation. Eucalyptus spp. Forests: Performance and Sensitivity. Forests, 15(1), p.209, DOI: 10.3390/f15010209.

Yin D. and Wang L. (2019). Individual mangrove tree measurement using UAV-based LiDAR data: Possibilities and challenges. Remote Sensing of Environment, 223, pp.34-49, DOI: 10.1016/j.rse.2018.12.034.

Yin D., Wang L., Lu Y. and Shi C. (2024). Mangrove tree height growth monitoring from multi-temporal UAV-LiDAR. Remote Sensing of Environment, 303, p.114002, DOI: 10.1016/j.rse.2024.114002.